We are IntechOpen, the world's leading publisher of Open Access books
Built by scientists, for scientists

5,600
Open access books available

137,000
International authors and editors

170M
Downloads

154
Countries delivered to

Our authors are among the

TOP 1%
most cited scientists

12.2%
Contributors from top 500 universities

CLARIVATE ANALYTICS
BOOK CITATION INDEX
INDEXED

WEB OF SCIENCE™

Selection of our books indexed in the Book Citation Index
in Web of Science™ Core Collection (BKCI)

Interested in publishing with us?
Contact book.department@intechopen.com

Numbers displayed above are based on latest data collected.
For more information visit www.intechopen.com

A Review on Convective Boiling Heat Transfer of Refrigerants in Horizontal Microfin-Tubes: A Typical Example

Thanh Nhan Phan and Van Hung Tran

Abstract

Understanding the Heat transfer performance of refrigerant for convective boiling in horizontal microfin tube and smooth tube is place an importance role on the designing of evaporator, the main equipment on refrigeration system. Reviewing the general concept especially the theory of boiling in the tube, the formation of the flow pattern map, the calculating procedure for heat transfer coefficient and pressure drop during boiling process of refrigerant in microfin tube. Besides, a typical example will be presented more detail in step by step to define the heat transfer coefficient and pressure drop for one working condition to estimate the data results without doing experiments.

Keywords: convective boiling, microfin tube, flow pattern, heat transfer coefficient, pressure drop

1. Introduction

The boiling process of Refrigerant is very important on the designing of evaporator on the refrigeration system. The optimization of heat exchanger about the size, weight and heat transfer performance is the main problem. In order to solve this problem, microfin tube is the ones should pay attention.

To understand the boiling process, the pattern of flow should be known during the boiling of refrigerant. With the type of flow patterns and the general map of flow pattern for boiling in smooth tube is very clear it is concluded fully stratified, slug flow, stratified wavy flow, intermittent flow, annular flow, dryout and mist flow. While for microfin is still unclear especially for the newest refrigerant. With the method of Rollmann et al. [1], the pattern of boiling in microfin tube could be classify in such fully stratified flow, stratified wavy flow, the combination of slug and stratified wavy flow, helix flow, annular flow. In order to build this method, Rollmann et al. was updated the method of Wojtan et al. [2] which was introduced for smooth tube. Those method based on the mathematical model of two phase stratified the geometries of flow from [3] to determine the geometries of flow. Besides that, in recent years some new method to build the map for flow pattern are still updated from Zhuang et al. [4] and Yang et al. [5].

In case of internal flow, the main difficulty, concerning to the evaluation of the heat transfer coefficient and friction factor, is related to the flow regimes (distribution of liquid and vapor in a cross-section). As it is easily understood, the main heat transfer mechanism changes if, at the wall, there is liquid, vapor, both of them, droplet impingement, bubble formation and so on. Every flow regime requires a specific analytical description and appropriate criteria to state if it occurs or not. As quality, liquid mass flux and vapor mass flux change along a duct, several flow regime onsets along a duct in the presence of heat transfer. The criteria are usually represented in two-dimensional diagrams called flow pattern maps. The internal geometry of the enhanced tubes and the thermal properties of the fluid affect the distribution of the phases in the cross section.

It is obviously that the outstanding performance of heat transfer in microfin tubes for boiling is valuable to consider without introducing excessive penalization in the pressure drop. Those have been proven in so many experimental researches which are published in recent years and also presented in the paper of Phan et al. [6]. Besides, with the correlations for heat transfer of evaporation process on microfin tube are published would be introduced in this chapter are come from Thome et al. [7], Cavallini et al. [8], Yu et al. [9], Yun et al. [10], Chamra et al. [11], Wu et al. [12], Rollmann and Spindle [13].

Also for the pressure drop of two phase flow, some correlations were built for both evaporation and condensation Choi et al. [14], Goto et al. [15], the others used for separated purposed. Some particular pressure drop correlations could be mentioned for evaporation Rollmann and Spindler [13], Wongsa-Ngam et al. [16] and Kuo et al. [17].

About this problem, Phan Thanh Nhan [18] focused on the experimental test to determine flow pattern, heat transfer and pressure drop for both boiling and condensation in microfin tube for two kind of Refrigerants R134a and R1234ze.

This chapter is demonstrated in convective boiling of refrigerant in horizontal microfin tube. Flow pattern map, heat transfer coefficient and pressure drop during boiling process would be presented with the published correlations and taken on working condition for boiling as an example to calculate step by step.

2. Flow pattern map

In order to draw a map of flow mechanism, there needs to be a classification of different regimes of flow in microfin tube, which relies on flow patterns such as slug, fully stratified, stratified wavy, helix, annular and some regimes are the combination of two or three flow pattern simultaneously happened. To build the map, many parameters have been cleared about geometries of tube, heat flux, mass flux, thermo-physical and thermodynamics properties of fluid, local quality, quality change of boiling processes and define the void fraction, Martineli parameter or also estimate the shape of flow (about the liquid part and vapor part consisted on the position of tube).

Even many different group researches, they also classified the map into some main regimes: bubbly flow, plug flow, slug flow, intermittent flow, stratified flow, stratified wavy flow, annular flow, dry-out regime, mist flow or transition regime, other differences just only the difference name they called for the same regime. Flow patterns in horizontal flows are illustrated in **Figure 1**. Depend on every single group they have every different name for their classification regimes. Every regime can be described as below:

- Bubbly flow: due to buoyancy force, gas bubbles focus on the upper part of tube, and normally take place at the high mass flow rate.

- Plug flow: the individual small bubbles have coalesced to create long bubble, can call the name elongated bubble flow.

- Slug flow: at high velocity, the wave amplitude is so large which increasing and touching to the top of the tube

- Intermittent flow: could be defined instead of plug and slug flow

- Fully stratified flow: at low velocity, liquid and vapor are completely separated, interface between them is smooth

- Stratified wavy flow: the formation of wave in the interface between liquid and vapor of stratified flow when the velocity of gas rises up

- Annular flow: when the liquid forms around perimeter of the tube, vapor flows in the core separate and make the annular shape of liquid flow.

- Dry-out regime: at higher quality of vapor, thinner of annular liquid flow will be disappeared, at the top of tube becomes dry first, then gradually spread around tube to bottom

- Mist flow: liquid will be entrained to the core of gas phase as small droplets

- Transition regime: on the changing pattern regimes, it is not clear to define which pattern they are, so that the name transition regime is used.

For micro-fin tube, those the last few years, some other detailed regimes are called for flow patterns:

- Helix flow: the formation of helix flow due to the helical structure of microfin where the liquid flow helically through out

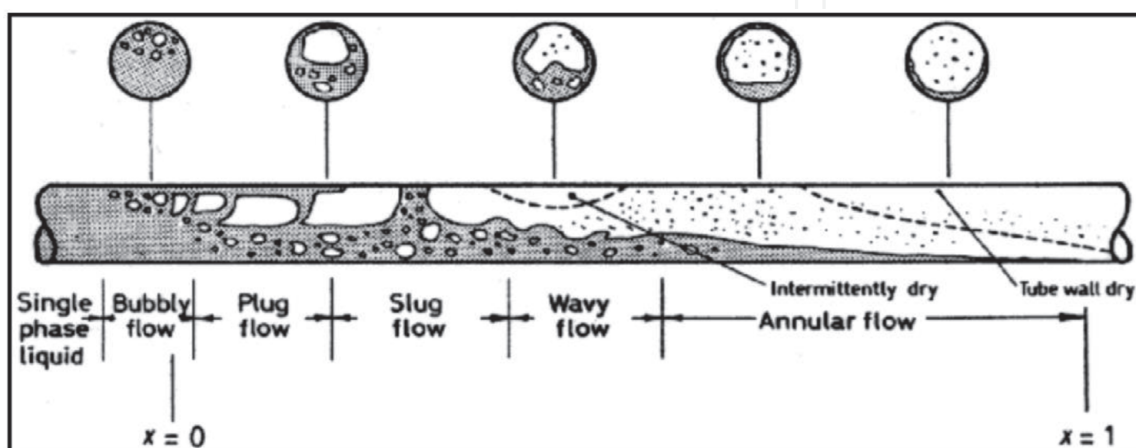- Slug + helix flow: on the regime, slug and helix flow are spontaneously occurred

Figure 1.
Flow regime for boiling from Collier and Thome 1994 [7].

2.1 The flow pattern map of Rollmann and Spindler

Rollmann and Spindler [1] modified the procedure from Wojtan et al. [2] and introduced their method to build the flow pattern map for boiling in microfin tube as given in below (**Figure 2**):

Void fraction ε: Rouhani-Axelsson correlation

$$\varepsilon = \frac{x}{\rho_V} \left([1 + 0.12(1-x)] \left[\left(\frac{x}{\rho_V} \right) + \left(\frac{1-x}{\rho_L} \right) \right] + \frac{1.18(1-x)[g\sigma(\rho_L - \rho_V)]^{0.25}}{G\rho_L^{0.5}} \right)^{-1}$$

(1)

Stratified angle θstrat: Biberg correlation [19]

$$\theta_{strat} = 2\pi - 2 \left\{ \pi(1-\varepsilon) + \left(\frac{3\pi}{2} \right)^{1/3} \left[1 - 2(1-\varepsilon) + (1-\varepsilon)^{\frac{1}{3}} - \varepsilon^{\frac{1}{3}} \right] \right.$$
$$\left. - \frac{1}{200}(1-\varepsilon)\varepsilon[1 - 2(1-\varepsilon)] \left[1 + 4\left((1-\varepsilon)^2 + \varepsilon^2\right) \right] \right\}$$

(2)

Geometrical parameters for two phase flow in a circular tube are showed in **Figure 3**.

$$A_{LD} = \frac{A_L}{D^2} = \frac{A(1-\varepsilon)}{D^2}$$

(3)

$$A_{VD} = \frac{A_V}{D^2} = \frac{A\varepsilon}{D^2}$$

(4)

Figure 2.
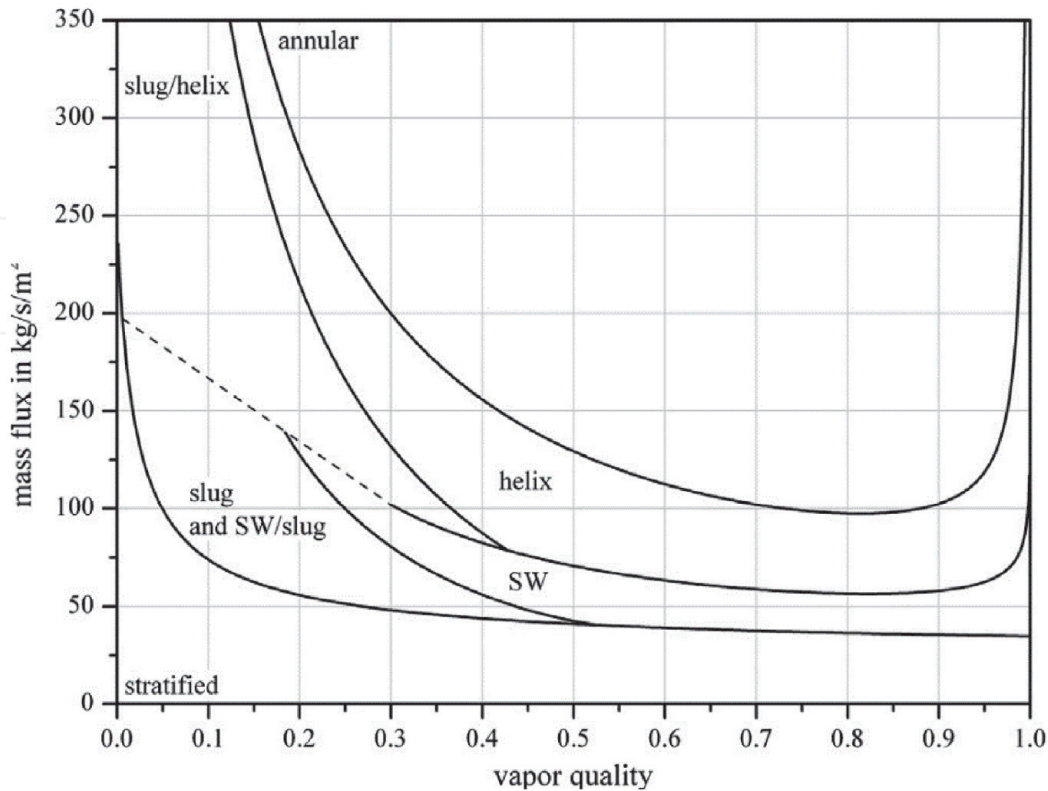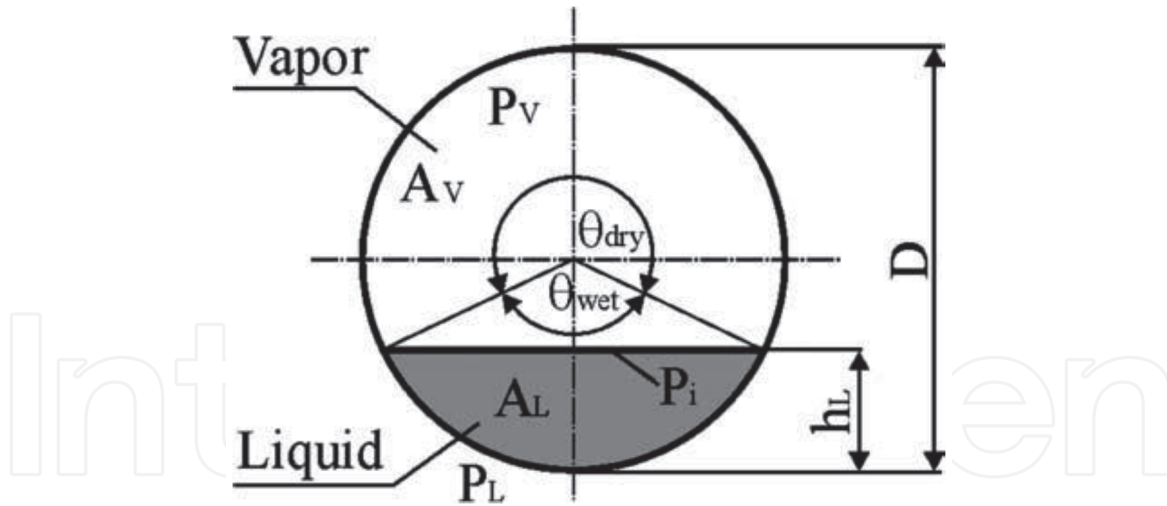*Flow pattern map of Rollmann and Spindle [1].*

Figure 3.
Geometrical parameters of stratified flow in circular tube.

$$h_{LD} = 0.5\left(1 - \cos\left(\frac{2\pi - \theta_{strat}}{2}\right)\right) \quad (5)$$

$$P_{iD} = \sin\left(\frac{2\pi - \theta_{strat}}{2}\right) \quad (6)$$

Transition between stratified flow and stratified wavy flow:

$$G_{strat} = \left\{\frac{4\mu_L g(\rho_L - \rho_V)\rho_V \varepsilon(1-\varepsilon)}{S_2 x^2(1-x)}\right\}^{1/3} + C_5; S_2 = 0.02844; C_5 = 22.9 \text{ kg/sm}^2. \quad (7)$$

Transition between slug flow and stratified wavy flow:

$$G_{slug} = \left\{\frac{16\widetilde{A_V^3}gD\rho_L\rho_V}{x^2\pi^2\sqrt{1-(2\widetilde{H_L}-1)^2}}C_6^2\left[\frac{4\pi^2}{S_1^2\widetilde{H_L}^2}\left(\frac{Fr}{We}\right)_L + 1\right]\right\}^{0.5} + C_7; \left(\frac{Fr}{We}\right)_L = \frac{\sigma}{gD^2\rho_L}; S_1$$
$$= 5.889; C_6 = 1.015; C_7 = -53.35\text{kg/sm}^2, \quad (8)$$

where H_L is liquid height, $\widetilde{H_L} = H_L/D$ and A_V is gas phase area, $\widetilde{A_V} = A_V/D$. Transition between stratified wavy flow and helix flow:

$$G_{SW} = \left\{\frac{16\widetilde{A_V^3}gD\rho_L\rho_V}{x^2\pi^2\sqrt{1-\left(2\widetilde{H_L}-1\right)^2}}C_6^2\right\}^{0.5} + C_7, \text{ for } x \geq 0.3; C_6 = 0.8441; C_7$$
$$= 0 \text{ kg/sm}^2. \quad (9)$$

For $x \geq 0.3$ the transition curve in Eq. (3) was applied. With $x < 0.3$ the linear equation With the lope of transition curve from $x \geq 0.3$.

Transition between slug/helix flow and helix flow:

$$G_{Slug-helix} = \left\{\frac{16\widetilde{A_V^3}gD\rho_L\rho_V}{x^2\pi^2\sqrt{1-\left(2\widetilde{H_L}-1\right)^2}}C_6^2\right\}^{0.5} + C_7; C_6 = 1.754; C_7$$
$$= -84.79 \text{ kg/sm}^2. \quad (10)$$

Transition between helix flow and annular flow:

$$G_{slug} = \left\{ \frac{16\widetilde{A_V^3}gD\rho_L\rho_V}{x^2\pi^2\sqrt{1-\left(2\widetilde{H_L}-1\right)^2}}C_6^2\left[\frac{4\pi^2}{S_1^2\widetilde{H_L}^2}\left(\frac{Fr}{We}\right)_L + 1\right]\right\}^{0.5} + C_7; S_1 = 57.71; C_6$$

$$= 1.772; C_7 = -25.39 \text{ kg/sm}^2.$$

(11)

The classification of the regimes on the map:

Conditions	Regime
$G < G_{strat}$	Stratified flow
$G > G_{slug}$ and $G < G_{sw}$	Stratified wavy flow
$G < G_{slug}$ and $G < G_{sw}$	Stratified wavy/slug flow or slug flow
$G < G_{slug-helix}$	Slug/helix flow
$G < G_{helix}$	Helix flow
$G > G_{helix}$	Annular flow

2.2 The flow pattern map of Zhuang et al.

The flow pattern map of Zhuang et al. [4] in **Figure 4** was form from the model of Kim et al. combine with their experimental data for R170 with working range of saturation pressures from 1.5 MPa to 2.5 MPa on mass flux from 100 kg/m^{2}s to 250 kg/m^{2}s. The map was built in the terms of dimensionless weber number We and Mattinelli parameter X_{tt}.
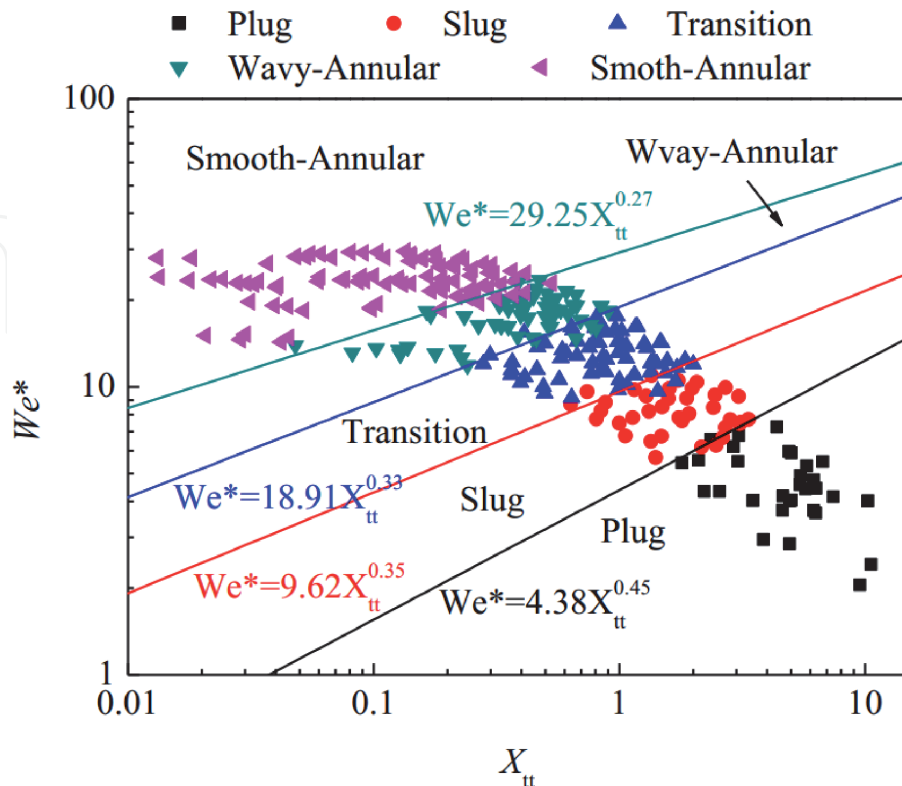

Figure 4.
Flow pattern map of Zhuang et al. [4].

Four transition curves were presented to draw the transition line to separate five different zones, each zone is named as smooth annular, wavy annular, transition, slug, plug.

Marttinelli number: X_{tt}

$$X_{tt} = \left(\frac{1-x}{x}\right)^{0.9}\left(\frac{\rho_G}{\rho_L}\right)^{0.5}\left(\frac{\mu_l}{\mu_G}\right)^{0.1} \tag{12}$$

Determine Weber number (We) based on the Reynold range of liquid flow:

$$Re_L = \frac{G(1-x)D}{\mu_L} \tag{13}$$

With $Re_L \leq 1250$

$$We^* = 2.45\frac{Re_G^{0.64}}{Su_G^{0.3}\left(1 + 1.09X_{tt}^{0.039}\right)^{0.4}} \tag{14}$$

With $Re_L > 1250$

$$We^* = 0.85\frac{Re_G^{0.79}X_{tt}^{0.157}}{Su_G^{0.3}\left(1 + 1.09X_{tt}^{0.039}\right)^{0.4}}\left[\left(\frac{\mu_G}{\mu_L}\right)^2\left(\frac{\rho_L}{\rho_G}\right)\right]^{0.084} \tag{15}$$

$$Su_G = \frac{\rho_G\sigma D}{\mu_G^2} \tag{16}$$

The transition line between patterns:
Smooth-annular to wavy-annular flow:

$$We^* = 29.25X_{tt}^{0.27} \tag{17}$$

Wavy-annular to transition flow:

$$We^* = 18.91X_{tt}^{0.33} \tag{18}$$

Transition to slug flow:

$$We^* = 9.62X_{tt}^{0.35} \tag{19}$$

Slug to plug flow:

$$We^* = 4.38X_{tt}^{0.45} \tag{20}$$

2.3 The flow pattern map of Yang et al.

The map of Yang et al. [5] introduced two maps in **Figure 5**, one map is presented for plug flow, slug flow, other is separate between slug flow and annular flow. Two transitions line on two difference maps as a function of Martinelli parameter X_{tt}, the transition lines based on three dimensionless numbers K_1, K_2, K_3 which depended on the inertia force, surface tension force, shear force, gravity force and evaporation momentum force.
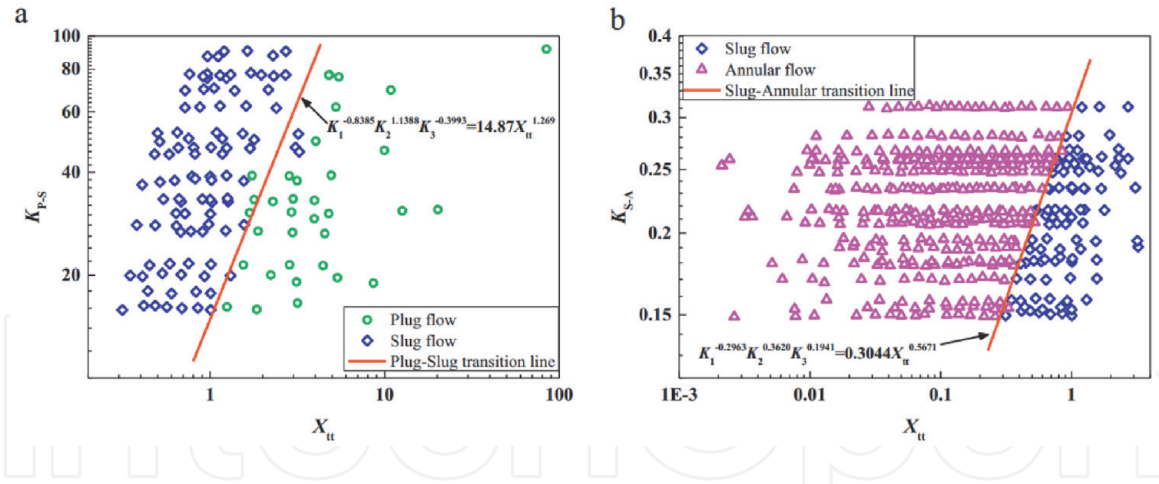
Figure 5.
Flow pattern map of Yang et al. [5].

Dimensionless number K1 is a ratio of evaporation momentum force with inertia force:

$$K_1 = \frac{\text{evaporation momentum force}}{\text{inertia force}} = \frac{\left(\frac{q}{h_{lv}}\right)^2 \frac{1}{\rho_v}}{\frac{G^2}{\rho_l}} = \left(\frac{q}{h_{lv}}\right)^2 \frac{\rho_l}{\rho_v} \qquad (21)$$

Dimensionless number K2 is a ratio of evaporation momentum force with surface tension force:

$$K_2 = \frac{\text{evaporation momentum force}}{\text{surface tension force}} = \frac{\left(\frac{q}{h_{lv}}\right)^2 \frac{1}{\rho_v}}{\frac{\sigma}{D}} = \left(\frac{q}{h_{lv}}\right)^2 \frac{D}{\sigma \rho_v} \qquad (22)$$

Dimensionless number K3 is a ratio of shear force with gravity force:

$$K_3 = \frac{\text{shear force}}{\text{gravity force}} = \frac{\frac{\mu_l}{\rho_l} \frac{G}{D}}{(\rho_l - \rho_v)gD} = \frac{\mu_l G}{(\rho_l - \rho_v)\rho_l g D^2} \qquad (23)$$

The transition line from plug to slug and slug to annular based on function of Xtt:
Plug to slug:

$$K = K_{P-S} = K_1^{-0.8385} K_2^{1.1388} K_3^{-0.3993} = 14.87 X_{tt}^{1.269} \qquad (24)$$

Slug to annular:

$$K = K_{S-A} = K_1^{-0.2963} K_2^{0.3620} K_3^{0.1941} = 0.3044 X_{tt}^{0.5671} \qquad (25)$$

3. Two phases heat transfer coefficient in boiling

Due to the changing phase during the convective boiling, the proportion of liquid and vapor is also changed, which affected the mechanism of boiling. In order to indicate the boiling heat transfer coefficient, the nucleate boiling and convective boiling are considered. More detailed about the methodology, the boiling number and some other factors are presented in the method of each group authors as below:

3.1 The correlation of Han et al.

Base on the basic form of boiling heat transfer coefficient, Han et al. [20] was established their correlation from the updating their experimental result. The experimental data results were done on the working range of mass flux G = [100; 250] kg/m²s, heat flux q = [11.76; 52.94] kW/m², temperature T = [−5, 8]°C with fluid R161 for microfin tube with 6.34 mm average inside diameter, 15° helix angle, 30° fin angle, 0.1 mm fin height, 65 number of fins.

Heat transfer coefficient of two-phase flow:

$$h_{r,tp} = Fh_{r,l} + Sh_{r,nb} \tag{26}$$

Convective heat transfer with convective fin factor:

$$h_{r,l} = E_{RB}h_l \tag{27}$$

$$h_l = 0.023 \, Re_l^{0.8} Fr_l^{0.4} \left(\frac{k_l}{d_i}\right) \tag{28}$$

$$E_{RB} = \left\{ 1 + \left[2.64 (Re_l)^{0.036} \left(\frac{e}{d_i}\right)^{0.212} \left(\frac{p}{d_i}\right)^{-0.21} \left(\frac{\beta}{90°}\right)^{0.29} (Pr_L)^{-0.024} \right]^7 \right\}^{1/7} \tag{29}$$

$$Re_{rl} = \frac{G(1-x)d_i}{\mu_l} \tag{30}$$

Heat transfer of nuclear boiling

$$h_{r,nb} = 55 P_r^{0.12} \left(- \log_{10} P_r\right)^{-0.55} M^{-0.5} q^{0.67} \tag{31}$$

The new function of F and S

$$F = 1 + aBo^{1.16} + b \left(\frac{1}{X_{tt}}\right)^{0.86} \tag{32}$$

$$S = \frac{1}{1 + cF^d \, Re_l^{1.17}} \tag{33}$$

In which a = 7196.741; b = 1.5135; c = 2.703; d = 1.94,
where e: microfin height; p: axial pitch from fin to fin; β: helix angle; N: number of fin; Pr: reduced pressure.

3.2 The correlation of Rollmann and Spindler

The model of Rollmann and Spindler [13] for heat transfer coefficient was derived with total 1614 data points experiment for refrigerant R407C on microfin tube at 8.95 mm fin root diameter, 0.24 mm fin height, 15° Helix angle, 25° Apex angle and 55 fins. Heat flux q = [1000; 20000] W/m², mass flux G = [25; 300] kg/m²s, saturation temperature Tsat = [−30; 10]°C,

The model defined by Nuselt number:

$$Nu(x, Bo, Re, Pr) = C_4 \left(\frac{C_1}{Pr^2} + C_2\right) Re^{2/3} [\ln(Bo) + C_3] x^{\left(\frac{C_1}{Pr^2} + C_2\right)} \tag{34}$$

where

$C_1 = -3.7$; $C_2 = 0.71$; $C_3 = 12.17$; $C_4 = 1.2$

$Bo = \frac{q}{G\Delta h_v}$; $Re = \frac{GD_{FR}}{\eta_L}$; $Pr = \frac{\eta_L C_{p,L}}{\lambda_L}$; $Nu = \frac{hD_{FR}}{\lambda_L}$

DFR: diameter at fin root

Working range: $Bo > 5.1837.10-6$; $Pr > 2.2828$

3.3 Correlation for boiling model of Chamra and Mago

The semi empirical model of Chamra and Mago [11] was derived based on 380 collected data points from available literature.

Working range of collected database	The range of microfin tube on database
Fluid: R134A, R12, R22, R123,	d_i = [7.92; 15.88] mm (inner tube diameter)
Ts = [0.6; 15]°C	n_f = [21; 100] number of microfin per unit length
q = [0; 64.3] kW/m²	e = [0.12; 0.38] mm (fin height)
x = [0.05; 1]	β = [10; 90]° (apex angle)
G = [25; 410] kg/m²s	γ = [3; 30]° (helix angle)
	L = [0.3-4.88] m
	t_h = [0.28-0.51] mm (tube wall thickness)

Developed on the basic of Cavallini model

$$h_{tp} = h_{pb}1.5160(X_{tt})^{1.1610}F_1^{-1.7640} + h_l\Phi Rx^{2.6220}(Bon^w Fr_V)^{-0.2158}F_2^{0.5927}F_3^{0.0582} \tag{35}$$

$$h_{pb} = 55P_R^{0.12}(-\log_{10}P_R)^{-0.55}M^{-0.5}q^{0.67} \tag{36}$$

$$q = G.i_{fg}.\Delta x \tag{37}$$

$$X_{tt} = \left(\frac{1-x}{x}\right)^{0.9}\left(\frac{\rho_v}{\rho_l}\right)^{0.5}\left(\frac{\mu_l}{\mu_v}\right)^{0.1} \text{ If } X_{tt} > 1 \text{ then } X_{tt} = 1 \tag{38}$$

$$F_1 = 0.01d_i^{-1} \tag{39}$$

$$h_l = 0.023\frac{k_l}{d_i}Re_l^{0.8}Pr_l^{0.4} \tag{40}$$

$$\Phi = \left[(1-x) + 2.63x\left(\frac{\rho_l}{\rho_v}\right)^{\frac{1}{2}}\right]^{0.8} \tag{41}$$

$$Rx = \left\{\frac{2en_f(1-\sin(\beta/2))}{\pi d_i\cos(\beta/2)} + 1\right\}\frac{1}{\cos(\gamma)} \tag{42}$$

$$Bon^w = \frac{g\rho_L e\pi d_i}{8\sigma n_f} \tag{43}$$

$$Fr_V = \frac{G^2}{\rho_v^2 g d_i} \tag{44}$$

$$F_2 = 0.01d_i^{-1} \tag{45}$$

$$F_3 = 100G^{-1} \tag{46}$$

3.4 The correlation of Yun et al.

Using the database with 749 data points of five different refrigerants to create a generalized correlation for boiling heat transfer in horizontal microfin tubes.

Heat transfer coefficient of two-phase flow:

$$h_{tp}/h_l = \left[C_1 Bo^{C_2} \left(\frac{P_{sat} d_i}{\sigma} \right)^{C_3} + C_4 \left(\frac{1}{X_{tt}} \right)^{C_5} \left(\frac{Gf}{\mu_l} \right)^{C_6} \right] Re_1^{C_7} Pr_1^{C_8} \left(\frac{\delta}{f} \right)^{C_9} \tag{47}$$

$$Bo = \frac{q}{Gh_{lv}} \tag{48}$$

$$h_l = 0.023 \, Re_1^{0.8} Fr_1^{0.4} \left(\frac{k_l}{d_i} \right) \tag{49}$$

$$Re_1 = \frac{G(1-x)d_i}{\mu_l} \tag{50}$$

$$\delta = \frac{d_r(1-\varepsilon)}{4} \tag{51}$$

$$\varepsilon = \frac{x}{\rho_G} \left[(1 + 0.12(1-x)) \left(\frac{x}{\rho_G} + \frac{1-x}{\rho_L} \right) + \frac{1.18(1-x)[g\sigma(\rho_L - \rho_G)]^{0.25}}{G\rho_L^{0.5}} \right]^{-1} \tag{52}$$

$$X_{tt} = \left(\frac{1-x}{x} \right)^{0.9} \left(\frac{\rho_v}{\rho_l} \right)^{0.5} \left(\frac{\mu_l}{\mu_v} \right)^{0.1} \tag{53}$$

Coefficients of correlation	The range of database
$C_1 = 0.009622$	d = [8.82; 14.66] mm (inner diameter)
$C_2 = 0.1106$	f = [0.12; 0.381] mm (fin height)
$C_3 = 0.3814$	spiral angle = [16; 30]°
$C_4 = 7.6850$	G = [50; 637] kg/m²s
$C_5 = 0.5100$	q = [5; 39.5] kW/m²
$C_6 = -0.7360$	Ts = [−15; 70]°C
$C_7 = 0.2045$	R22, R113, R123, R134A, R410A
$C_8 = 0.7452$	
$C_9 = -0.1302$	
d_i: maximum inside diameter of a microfin tube	
d_r: diameter of a microfin tube at fin root	

3.5 The correlation of Cavallini et al.

The correlation of Cavallini et al. [8] produced for not only microfin tube but also for cross groves tubes with 643 data points collected from available literatures.

Heat transfer coefficient of two phase flow:

$$\alpha = \alpha_{nb} + \alpha_{cv} \tag{54}$$

Nucleate boiling component:

$$\alpha_{nb} = \alpha_{cooper} S.F_1(d_i) = \left[55 P_R^{0.12} \left(-\log_{10} P_R \right)^{-0.55} M^{-0.5} q^{0.67} \right] S.F_1(d_i) \tag{55}$$

$$S = A.X_{tt}^B = A. \left[\left(\frac{1-x}{x} \right)^{0.9} \left(\frac{\rho_G}{\rho_L} \right)^{0.5} \left(\frac{\mu_L}{\mu_G} \right)^{0.1} \right]^B \quad \text{If } X_{tt} > 1 \text{ then } X_{tt} = 1 \tag{56}$$

$F_1(d_i)$: function of fin tip tube diameter

$$F_1(d_i) = \left(\frac{d_o}{d_i}\right)^C \tag{57}$$

Convective term:

$$\alpha_{cv} = \frac{\lambda_L}{d_i}.Nu_{cv,\text{smooth tube}}.Rx^S.(Bo.Fr)^T.F_2(d_i).F_3(G) \tag{58}$$

$$Nu_{cv,\text{smooth tube}} = Nu_{LO}\Phi = \left[0.023\left(\frac{Gd_i}{\mu_L}\right)^{0.8}Pr_L^{1/3}\right]\left[(1-x)+2.63x\left(\frac{\rho_L}{\rho_G}\right)^{1/2}\right]^{0.8} \tag{59}$$

$$Rx = \left\{\frac{2hn_g(1-\sin{(\gamma/2)})}{\pi d_i\cos{(\gamma/2)}}+1\right\}\frac{1}{\cos{(\beta)}} \tag{60}$$

$$Bo = \frac{g\rho_L h\pi d_i}{8\sigma n_g} \tag{61}$$

$$Fr = \frac{u_{GO}{}^2}{gd_i} \tag{62}$$

$$F_2(d_i) = \left(\frac{d_o}{d_i}\right)^V \tag{63}$$

$$F_3(G) = \left(\frac{G_o}{G}\right)^Z \tag{64}$$

u_{GO}: velocity of gas phase with total flow rate

	A	B	C	S	T	V	Z	do	Go
G < 500 kg/m²s	1.36	0.36	0.38	2.14	−0.15	0.59	0.36	0.01	100
G ≥ 500 kg/m²s	1.36	0.36	0.38	2.14	−0.21	0.59	0.36	0.01	100

Working range:

Geometry of tubes:	Experimental Data bank: 643
d_i = [3; 14.3] mm (minimum inside tube diameter)	Fluid: R134A, R12, R22, R123, R125, R32
ng = [30; 112] (number of grooves)	Ts = [−6.6; 48]°C
h = [0.1; 0.35] mm (fin height)	q = [3; 82] kW/m²
γ = [20; 120]° (apex angle)	x = [0.05; 0.9]
β = [4; 30]° (spiral angle)	G = [90; 600] kg/m²s
L = [0.2; 3.67] m	

3.6 The correlation of Thome et al.

The model was derived to predict the microfin with the test data for R134a, R123, mass flux G = [100; 500] kg/m²s, quality x = [0.15; 0.85] and heat flux q = [2; 47] kW/m²

$$h = E_{mf}\left[(h_{nb})^3+(E_{RB}h_{cv})^3\right]^{1/3} \tag{65}$$

$$h_{nb} = 55P_R^{0.12}\left(-\log_{10}P_R\right)^{-0.55}M^{-0.5}q^{0.67} \tag{66}$$

$$h_{cv} = 0.0133\,Re_l^{0.69}Pr_l^{0.4}\lambda_l/\delta \tag{67}$$

$$(Re_l)_{film} = \frac{4G(1-x)\delta}{(1-\epsilon)\mu_l} \tag{68}$$

$$\delta = d_r(1-\epsilon)/4 \tag{69}$$

$$\epsilon = \frac{x}{\rho_G}\left[(1+0.12(1-x))\left(\frac{x}{\rho_G}+\frac{1-x}{\rho_L}\right) + \frac{1.18(1-x)[g\sigma(\rho_L-\rho_G)]^{0.25}}{G\rho_L^{0.5}}\right]^{-1} \tag{70}$$

$$E_{mf} = 1.89\left(\frac{G}{G_{ref}}\right)^2 - 3.7\left(\frac{G}{G_{ref}}\right) + 3.02 \tag{71}$$

$$E_{RB} = \left\{1 + \left[2.64(Re_D)^{0.036}\left(\frac{e}{d_r}\right)^{0.212}\left(\frac{p}{d_r}\right)^{-0.21}\left(\frac{\beta}{90^\circ}\right)^{0.29}(Pr_L)^{-0.024}\right]^7\right\}^{1/7} \tag{72}$$

$$Re_D = \frac{G(1-x)d_r}{\mu_l} \tag{73}$$

$$p = \frac{\pi d_r/N}{\tan\beta} \tag{74}$$

$$G_{ref} = 500\,kg/m^2s \tag{75}$$

where e: microfin height; p: axial pitch from fin to fin; β: helix angle; N: number of fins; dr: root diameter

4. Pressure drop

4.1 The correlation of Choi et al.

The model form of Choi et al. [14] was carryout from Pierre 1964 model with 831 data pointed collected from NIST database with 626 data point for boiling and 205 data points for condensation for some different fluids R134a, R22, R125, R32, R407C, R410A and R32/R134a. Those data points derived with test section has 8.92 mm root diameter, 9.52 mm outside diameter, 18° helix angle.

Total pressure drop:

$$\frac{\Delta p}{L} = \frac{\Delta p_f}{L} + \frac{\Delta p_m}{L} = G^2\left[f\frac{(v_{tp,out}+v_{tp,in})}{d_h} + \frac{(v_{tp,out}-v_{tp,in})}{L}\right] \tag{76}$$

Two phase friction factor:

$$f = 0.00506\,Re_{h,LO}^{-0.0951}K_f^{0.1554} \tag{77}$$

$$Re_{h,LO} = Gd_h/\mu_l \tag{78}$$

Hydraulic diameter:

$$d_h = 4A_c\cos\beta/(n.S_p) \tag{79}$$

Two phase number:

$$K_f = \frac{\Delta x . h_{lv}}{gL} \tag{80}$$

"Specific volumes of the two-phase fluid, $v_{tp,out}$ and $v_{tp,in}$, are quality-weighted sums of the vapor and liquid specific volumes at either the outlet or inlet of the tube"

4.2 The correlation of Goto et al.

Model of Goto et al. [15] derived from experiment of R41A and R22 for both boiling and condensation at mass flux G = [200; 340] kg/m²s inside spiral groove tube 7.3 mm mean inside diameter and herring-born groove tube 7.24 mm mean inside diameter.

Frictional pressure gradient:

$$\left(\frac{dP}{dz}\right)_f = \Phi_v^2 \left(\frac{dP}{dz}\right)_v = \Phi_v^2 2 f_{e,v,Go} (Gx)^2 / (\rho_v d_e) \tag{81}$$

$$\Phi_v = 1 + 1.64 X_{tt}^{0.79} \tag{82}$$

Or could be compute based on the liquid phase form

$$\left(\frac{dP}{dz}\right)_f = \Phi_l^2 \left(\frac{dP}{dz}\right)_l = \Phi_l^2 2 f_{e,l,Lo} (G(1-x))^2 / (\rho_l d_e) \tag{83}$$

$$\Phi_l = 1 + 7.61 X_{tt}^{-1.7} \tag{84}$$

$$Re_{e,v} = Gx d_e / \mu_v \quad \text{Diameter of inner tube de} \tag{85}$$

$$X_{tt} = \left(\frac{1-x}{x}\right)^{0.9} \left(\frac{\rho_v}{\rho_l}\right)^{0.5} \left(\frac{\mu_l}{\mu_v}\right)^{0.1} \tag{86}$$

$$Re_{e,v} \leq 2000; => f_{e,v,Go} = 16 / Re_{e,v} \tag{87}$$

$$2000 \leq Re_{e,v} \leq 2600; => f_{e,v,Go} = 0.000147 \, Re_{e,v}^{0.53} \tag{88}$$

$$2600 \leq Re_{e,v} \leq 6500; => f_{e,v,Go} = 0.046 \, Re_{e,v}^{-0.2} \tag{89}$$

$$6500 \leq Re_{e,v} \leq 12700; => f_{e,v,Go} = 0.00123 \, Re_{e,v}^{0.21} \tag{90}$$

$$12700 \leq Re_{e,v}; => f_{e,v,Go} = 0.0092 \tag{91}$$

4.3 The correlation of Wongsa et al.

The correlation for boiling with high mass flux was proposed by Wongsa et al. [16]. Derived from their experimental results for R134a on microfin tube with 8.92 mm inner diameter, saturation temperature Tsat = [10; 20]°C, mass flux G = [400; 800] kg/m²s.

Two phase friction pressure drop

$$\left(\frac{dP}{dz}\right)_f = \Phi_{VO}^2 \left(\frac{dP}{dz}\right)_{h,VO} = \Phi_{VO}^2 2 f_{h,VO} G^2 / (\rho_v d_h) \tag{92}$$

$$4 f_{h,VO} = \frac{1.325}{\left[\ln \left(\frac{R x_h}{3.7} + \frac{5.74}{Re_{h,VO}^{0.9}} \right) \right]^2} \tag{93}$$

$$Re_{h,VO} = \frac{Gd_h}{\mu_v} \tag{94}$$

$$Rx_h = \frac{0.3(e/d_h)}{(0.1 + \cos\beta)} \tag{95}$$

$$\Phi_{VO}^2 = 2.3263 - 1.8043 \left\{ \frac{X_{tt}G}{[gd_h\rho_v(\rho_l - \rho_v)]^{0.5}} \right\}^{0.0802} \tag{96}$$

4.4 The correlation of Kou and Wang

The correlation of Kou and Wang 1996 [17] was analyzed from their own experimental data results for boiling of R22 and R407C in a 9.52 mm diameter micro-fin tube and a smooth tube at two different evaporation temperatures (6°C and 10°C). The mass flux was between 100 and 300 kg/m^{2}s and the heat fluxes 6 and 14 kW/m^2.

$$\left(\frac{dP}{dz}\right)_f = \frac{0.0254G^2[xv_v + (1-x)v_l]}{d_{fr}} \tag{97}$$

5. Example

Determine the heat transfer coefficient and pressure drop of refrigerant R1234ze during boiling process inside horizontal microfin tube at 5°C and heat flux 8,62 kW/m^2, mass flux 222 kg/m^{2}s. The geometry of microfin tube is 60 number of fins, the inner surface diameter is 8.96 mm, fin height is 0.2 mm, the helix angle and apex angle are 18° and 40°, respectively.

Solve:

At saturation temperature t_{sat} = 5°C of refrigerant R1234ze, thermal properties could be taken in **Table 1**.

Refrigerant: R1234ze, molar mass: M = 114 g/mol, $p_{critical}$ = 3.64 MPa
Reduce pressure: p_r = $p_{sat}/p_{critical}$ = 0.2593/3.64 = 0.07124
Heat flux: q = 8.62 kW/m^2
Mass flux: G = 222 kg/m^{2}s
Microfin tube: N = 60 number of fins, dr = 8.96 mm, e = 0.2 mm, β = 18o; γ = 40°

Property	Unit	Value	Property	Unit	Value
T_{sat}	[°C]	5	P_{sat}	[MPa]	0.2593
ρ_L	[kg/m^3]	1225.5	λ_L	[W/m-K]	8.14E-02
ρ_V	[kg/m^3]	13.9	λ_V	[W/m-K]	1.20E-02
ν_L	[m^3/kg]	8.16E-04	μ_L	[Pa-s]	2.53E-04
ν_v	[m^3/kg]	7.18E-02	μ_V	[Pa-s]	1.14E-05
hL_V	[kJ/kg]	181	Pr_L	[−]	4.102
Cp_L	[kJ/kg-K]	1.319	Pr_V	[−]	0.86
Cp_V	[kJ/kg-K]	0.898	σ	[N/m]	1.15E-02

Table 1.
Properties of R1234ze.

5.1 Flow pattern map

Apply the flow pattern map of Rollmann and Spindler [1] to present in here. At first, calculate the transition lines between one regime to another as a function of quality x and use the classification of the regimes on the map:

Conditions	Regime
$G < G_{strat}$	Stratified flow
$G > G_{slug}$ and $G < G_{sw}$	Stratified wavy flow
$G < G_{slug}$ and $G < G_{sw}$	Stratified wavy/slug flow or slug flow
$G < G_{slug-helix}$	Slug/helix flow
$G < G_{helix}$	Helix flow
$G > G_{helix}$	Annular flow

In this case, the flow pattern map for boiling of R1234ze in microfin tube was built at 5 °C saturation temperature, heat flux q = 8.62 kW/m^2, with the fixed mass flux G = 222 kg/m^{2}s.

The result map shown in **Figure 6**, when the mass flux lower than 50 kg/m^{2}s, the flow boiling during the changing phase just only occur at the fully stratified flow. But if working condition at mass flux 200 kg/m^{2}s, at the beginning of boiling process, the quality is still low, the boiling occur at slug/helix flow until the quality reach to 0.15, the helix flow happen, and keep boiling with the helix flow until quality is 0.25, it moves to the annular flow boiling to the rest of changing phase.
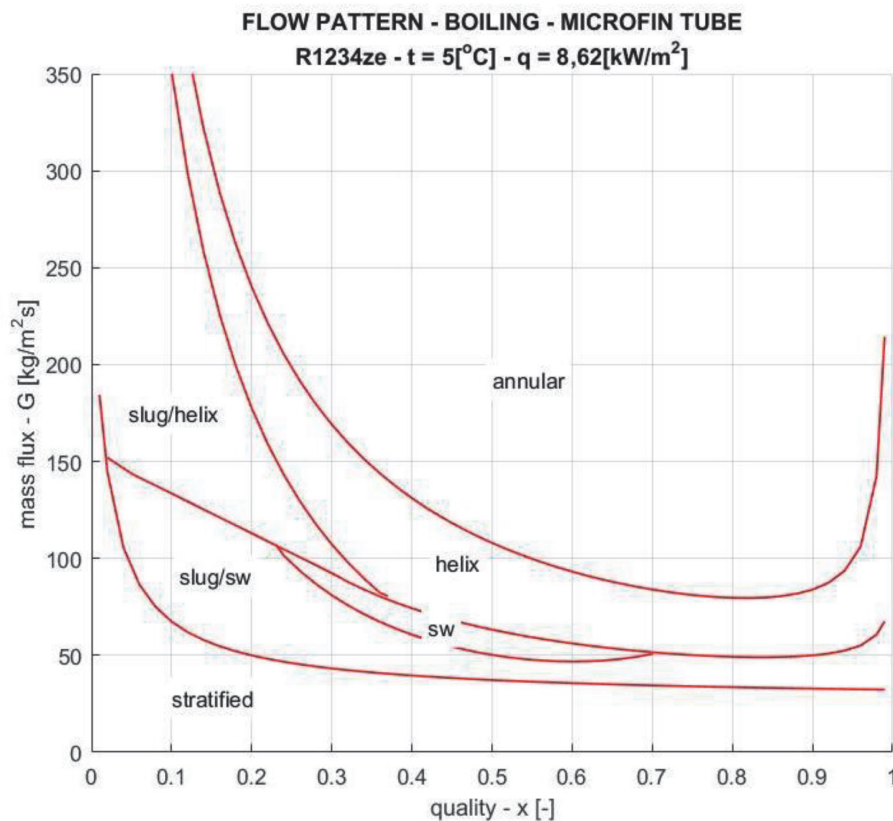

Figure 6.
Flow pattern map on microfin tube.

5.2 Heat transfer coefficients

Could take quality x = 0.5 as an example to present the procedure to calculate heat transfer coefficient and pressure drop of boiling refrigerant inside horizontal microfin tube, with the data point of quality x from 0 to 1 can be determined with the same method.

5.2.1 Applied the correlation of Thome et al.

Apply equation from (65) to (75) to calculate heat transfer coefficients as below: Void fraction

$$\varepsilon = \frac{x}{\rho_G}\left[(1+0.12(1-x))\left(\frac{x}{\rho_G}+\frac{1-x}{\rho_L}\right)+\frac{1.18(1-x)[g\sigma(\rho_L-\rho_G)]^{0.25}}{G\rho_L^{0.5}}\right]^{-1}$$

$$\varepsilon = \frac{0.5}{13.9}\left[(1+0.12(1-0.5))\left(\frac{0.5}{13.9}+\frac{1-0.5}{1225.5}\right)+\frac{1.18(1-0.5)[9.81x0.0115(1225.5-13.9)]^{0.25}}{222x1225.5^{0.5}}\right]^{-1}$$

$$\varepsilon = 0.9266$$

$$\delta = \frac{d_r(1-\varepsilon)}{4} = \frac{8.96.10^{-3}(1-0.9266)}{4} = 0.00016m$$

$$Re_1 = \frac{4G(1-x)\delta}{(1-\varepsilon)\mu_l} = \frac{4x222x(1-0.5)x0.00016}{(1-0.9266)x0.000253} = 3931.067$$

$$h_{cv} = \frac{0.0133\,Re_l^{0.69}Pr_l^{0.4}\lambda_l}{\delta} = \frac{0.0133(3931.067^{0.69})(4.102^{0.4})0.0814}{0.00016} = 3497.97$$

$$h_{nb} = 55P_R^{0.12}(-\log_{10}P_R)^{-0.55}M^{-0.5}q^{0.67}$$
$$= 55x0.07124^{0.12}(-\log_{10}0.07124)^{-0.55}114^{-0.5}8620^{0.67} = 1507.309$$

$$G_{ref} = 500kg/m^2s$$

$$E_{mf} = 1.89\left(\frac{G}{G_{ref}}\right)^2 - 3.7\left(\frac{G}{G_{ref}}\right) + 3.02 = 1.89\left(\frac{222}{500}\right)^2 - 3.7\left(\frac{222}{500}\right) + 3.02 = 1.75$$

$$Re_D = \frac{G(1-x)d_r}{\mu_l} = \frac{222(1-0.5)0.00896}{0.000253} = 3931.07$$

$$p = \frac{\pi d_r/N}{\tan\beta} = \frac{\pi x 0.00896/60}{\tan(18°)} = 0.001444$$

$$E_{RB} = \left\{1+\left[2.64(Re_D)^{0.036}\left(\frac{e}{d_r}\right)^{0.212}\left(\frac{p}{d_r}\right)^{-0.21}\left(\frac{\beta}{90°}\right)^{0.29}(Pr_L)^{-0.024}\right]^7\right\}^{1/7} = 1.43$$

$$E_{RB} = \left\{1+\left[2.64(3931.07)^{0.036}\left(\frac{0.0002}{0.00896}\right)^{0.212}\left(\frac{0.001444}{0.00896}\right)^{-0.21}\left(\frac{18°}{90°}\right)^{0.29}(4.102)^{-0.024}\right]^7\right\}^{1/7}$$

$$E_{RB} = 1.43$$

$$h = E_{mf}\left[(h_{nb})^3 + (E_{RB}h_{cv})^3\right]^{1/3} = 1.75\left[(1507.309)^3 + (1.43x3497.97)^3\right]^{1/3}$$
$$= 8831.04\left(\frac{W}{m^2K}\right)$$

5.3 Pressure drop

5.3.1 The correlation of Goto et al.

Apply equation from (81) to (91) to calculate pressure drop as below:
Frictional pressure gradient:

$$\left(\frac{dP}{dz}\right)_f = \Phi_v^2 \left(\frac{dP}{dz}\right)_v = \Phi_v^2 2f_{e,v,Go}(Gx)^2/(\rho_v d_e)$$

$$X_{tt} = \left(\frac{1-x}{x}\right)^{0.9}\left(\frac{\rho_v}{\rho_l}\right)^{0.5}\left(\frac{\mu_l}{\mu_v}\right)^{0.1} = \left(\frac{1-0.5}{0.5}\right)^{0.9}\left(\frac{13.9}{1225.5}\right)^{0.5}\left(\frac{0.000253}{0.0000114}\right)^{0.1}$$
$$= 0.1452$$

$$\Phi_v = 1 + 1.64X_{tt}^{0.79} = 1 + 1.640x1452^{0.79} = 1.3571$$

$$Re_{e,v} = \frac{G.x.d_e}{\mu_v} = \frac{222x0.5x0.00896}{0.0000114} = 87242.11$$

Compare $Re_{e,v}$ to get $f_{e,v,Go}$

$$Re_{e,v} \leq 2000; => f_{e,v,Go} = 16/Re_{e,v}$$

$$2000 \leq Re_{e,v} \leq 2600; => f_{e,v,Go} = 0.000147\,Re_{e,v}^{0.53}$$

x [−]	h [W/m2s]	dP/dz. [Pa/m]
0.01	2807.2	78.0
0.05	3640.1	248.5
0.10	4712.6	532.1
0.15	5561.5	811.6
0.20	6234.6	1115.3
0.25	6789.2	1441.7
0.30	7265.0	1789.0
0.35	7689.4	2155.5
0.40	8082.1	2539.5
0.45	8458.3	2939.1
0.50	8831.0	3352.5
0.55	9212.8	3777.6
0.60	9617.1	4212.3
0.65	10060.3	4653.8
0.70	10564.8	5099.2
0.75	11164.6	5544.6
0.80	11917.8	5984.8
0.85	12938.2	6412.2
0.90	14500.7	6814.0
0.95	17596.5	7162.5
0.99	27601.3	7331.9

Table 2.
Heat transfer coefficient and pressure drop during the boiling process.

$$2600 \leq \text{Re}_{e,v} \leq 6500; \; => f_{e,v,Go} = 0.046\,\text{Re}_{e,v}^{-0.2}$$

$$6500 \leq \text{Re}_{e,v} \leq 12700; \; => f_{e,v,Go} = 0.00123\,\text{Re}_{e,v}^{0.21}$$

$$12700 \leq \text{Re}_{e,v}; \; => f_{e,v,Go} = 0.0092$$

With $12700 \leq \text{Re}_{e,v} = 87242.11; \; => f_{e,v,Go} = 0.0092$

$$\left(\frac{dP}{dz}\right)_f = \Phi_v^2 \left(\frac{dP}{dz}\right)_v = \frac{\Phi_v^2 2 f_{e,v,Go}(Gx)^2}{(\rho_v d_e)} = \frac{(1.3571)^2 x 2x (0.0092)(222x0.5)^2}{(13.9x0.00896)}$$
$$= 3352.52 \left(\frac{Pa}{m}\right)$$

Apply the same procedure at each data point of quality x of refrigerant from 0.1 to 0.99 to determine heat transfer and pressure drop during the convective boiling. Data results are obtained in **Table 2**.

6. Conclusions

This chapter is presented the boiling process of refrigerant in horizontal microfin tube. Those are related to the understanding of flow patterns and the procedure to build some flow pattern maps. Some of new correlations to calculate heat transfer coefficient and pressure drop of refrigerant during boiling process have been presented. Detailed step by step to calculate heat transfer performance for typical example is also introduced. However, this is still not enough for this topic, with the new structure of microfin tubes, new refrigerants, this just only the general method to estimate the value, it should be confirmed by experimental method and create the new correlation to extend the wide range of application working conditions.

Acknowledgements

Author details

Thanh Nhan Phan[1,2*] and Van Hung Tran[1,2]

1 Ho Chi Minh City University of Technology (HCMUT), Ho Chi Minh City, Vietnam

2 Vietnam National University Ho Chi Minh City, Linh Trung Ward, Thu Duc District, Ho Chi Minh City, Vietnam

*Address all correspondence to: phannhan@hcmut.edu.vn

IntechOpen

References

[1] P. Rollmann and K. Spindler, "A new flow pattern map for flow boiling in microfin tubes," Int. J. Multiph. Flow, vol. 72, pp. 181–187, 2015.

[2] L. Wojtan, T. Ursenbacher, and J. R. Thome, "Investigation of flow boiling in horizontal tubes: Part I - A new diabatic two-phase flow pattern map," Int. J. Heat Mass Transf., vol. 48, no. 14, pp. 2955–2969, 2005.

[3] D. Biberg, "a Mathematical Model for Two-Phase Stratified Turbulent Duct Flow," Multiph. Sci. Technol., vol. 19, no. 1, pp. 1–48, 2007.

[4] X. Zhuang, M. Gong, G. Chen, X. Zou, and J. Shen, "Two-phase flow pattern map for R170 in a horizontal smooth tube," Int. J. Heat Mass Transf., vol. 102, pp. 1141–1149, 2016.

[5] Z. Q. Yang *et al.*, "A new flow pattern map for flow boiling of R1234ze(E) in a horizontal tube," Int. J. Multiph. Flow, vol. 98, pp. 24–35, 2018.

[6] Thanh Nhan Phan, Van Hung Tran, Nilola Kaloyanov and Momchil Vassilev, "Heat transfer performance of R1234yf for convective boiling in horizontal micro-fin and smooth tubes," E3s Web of Conference 207, vol. 9, 2020.

[7] J. R. Thome, D. Favrat, and N. Kattan, "Evaporation in microfin tubes: A generalized prediction model," *Proc. Convect. Flow Pool Boil. Conf.*, no. May, 1997.

[8] A. Cavallini, D. Del Col, L. Doretti, G. A. Longo, and L. Rossetto, "Refrigerant vaporization inside enhanced tubes: A heat transfer model," Heat Technol., vol. 17, no. 2, pp. 29–36, 1999.

[9] M. Yu, T. Lin, and C. Tseng, "Heat transfer and flow pattern during two-phase flow boiling of R-134a in horizontal smooth and microfin tubes ´

coulement lors de l ' e ´ bullition R134a : transfert de chaleur et e ´ coulement diphasique sur des tubes horizontaux lisses et a en e microa," vol. 25, pp. 789–798, 2002.

[10] R. Yun, Y. Kim, K. Seo, and H. Young Kim, "A generalized correlation for evaporation heat transfer of refrigerants in micro-fin tubes," Int. J. Heat Mass Transf., vol. 45, no. 10, pp. 2003–2010, 2002.

[11] L. M. Chamra and P. J. Mago, "Modelling of evaporation heat transfer of pure refrigerants and refrigerant mixtures in microfin tubes," Proc. Inst. Mech. Eng. Part C J. Mech. Eng. Sci., vol. 221, no. 4, pp. 443–454, 2007.

[12] Z. Wu, Y. Wu, B. Sundén, and W. Li, "Convective vaporization in micro-fin tubes of different geometries," Exp. Therm. Fluid Sci., vol. 44, pp. 398–408, 2013.

[13] P. Rollmann and K. Spindler, "New models for heat transfer and pressure drop during flow boiling of R407C and R410A in a horizontal microfin tube," Int. J. Therm. Sci., vol. 103, pp. 57–66, 2016.

[14] J. Y. Choi, M. a Kedzierski, and P. a Domanski, "Generalized Pressure Drop Correlation for Evaporation and Condensation in Smooth and Micro-Fin Tubes," no. 1 986, 2001.

[15] N. I. M. Goto, N. Inoue, "Condensation and evaporation heat transfer of R410A inside internally grooved horizontal tubes," Int. J. Refrig., vol. 24, no. 1, pp. 528–538, 2001.

[16] J. Wongsa-Ngam, T. Nualboonrueng, and S. Wongwises, "Performance of smooth and micro-fin tubes in high mass flux region of R-134a during evaporation," *Heat Mass Transf. und Stoffuebertragung*, 2004.

[17] C. S. Kuo and R. Laboratories, "In-tube evaporation of HCFC-22 in a 9. 52 mm micro-fin / smooth tube," *Science (80-.).*, vol. 39, no. 12, 1996.

[18] Phan Thanh Nhan, Pressure drop, heat transfer and flow pattern maps inside smooth and enhanced tubes during convective boiling and condensation of R134a and R1234ze [thesis]. Milan, Italy: Politecnical di Milano; 2019.

[19] D. Biberg, "An explicit approximation for the wetted angle in two-phase stratified pipe flow," Can. J. Chem. Eng., vol. 77, no. 6, pp. 1221–1224, 1999.

[20] X. H. Han, Y. B. Fang, M. Wu, X. G. Qiao, and G. M. Chen, "Study on flow boiling heat transfer characteristics of R161/oil mixture inside horizontal micro-fin tube," Int. J. Heat Mass Transf., vol. 104, pp. 276–287, 2017.